Eur. Phys. J. C 5, 111–117 (1998)
DOI 10.1007/s100529800820

THE EUROPEAN PHYSICAL JOURNAL C
© Springer-Verlag 1998

Structure functions of nuclei at small x and diffraction at HERA

A. Capella, A. Kaidalov[a], C. Merino[b], D. Pertermann[c], J. Tran Thanh Van

Laboratoire de Physique Théorique et Hautes Energies [d], Université de Paris XI, bâtiment 211, F-91405 Orsay cedex, France

Received: 25 September 1997 / Published online: 26 February 1998

Abstract. Gribov theory is applied to investigate the shadowing effects in the structure functions of nuclei. In this approach these effects are related to the process of diffractive dissociation of a virtual photon. A model for this diffractive process, which describes well the HERA data, is used to calculate the shadowing in nuclear structure functions. A reasonable description of the x, Q^2 and A-dependence of nuclear shadowing is achieved.

1 Introduction

Deep inelastic scattering (DIS) on nuclei gives important information on distributions of quarks and gluons in nuclei. The region of small Bjorken x is especially interesting because partonic clouds of different nucleons overlap as $x \to 0$ and shadowing effects become important. There are experimental results in this region, which show that there are strong deviations from an A^1 behavior in the structure functions [1]. Several theoretical models have been proposed to understand these data [1]. The most general approach is based on the Gribov theory [2]. It relates partonic and hadronic descriptions of small x phenomena in interactions of real or virtual photons with nuclei. In this approach the shadowing effects can be expressed in terms of the cross-sections for diffraction dissociation of a photon on a nucleon (Fig. 1). This process has been studied recently in DIS at HERA [3]. The detailed x, Q^2 and M^2 (M is the invariant mass of the diffractively produced system) dependencies observed in these experiments have been well described in the theoretical model of [4] which is based on Regge factorizations and uses as an input available information on diffractive production in hadronic interactions. Here we will apply the same model to calculate the structure functions of nuclei in the small x-region. The use of the model, which describes well the diffraction dissociation of virtual photons on a nucleon target, leads to a strong reduction of the theoretical uncertainty in calculations of the structure functions of nuclei in comparison with previous calculations [1, 5–8]. It also allows to discuss the shadowing effects in gluon distributions.

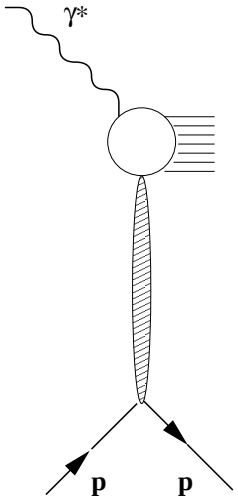

Fig. 1. Diffractive dissociation of a virtual photon. The *shaded area* represents the exchange of a Pomeron

2 The model

In the Gribov approach the forward scattering amplitude of a photon with virtuality Q^2 on a nuclear target can be written as the sum of the diagrams shown in Fig. 2. Since we are interested in the low x region we will describe the various $\gamma^* N$ interactions by Pomeron exchange. The diagram of Fig. 2a corresponds to the sum of interactions with individual nucleons and is propotional to A^1. The second diagram (2b) contains a double scattering with two target nucleons. It gives a negative contribution to the total cross-section, proportional to $A^{4/3}$ (for large A). It describes the first shadowing correction for sea quarks. According to reggeon diagram technique [9] and Abramovsky, Gribov, Kancheli (AGK) cutting rules

[a] *Permanent address:* ITEP, B. Cheremushkinskaya 25, 117259 Moscow, Russia

[b] *Permanent address:* Universidade Santiago de Compostela, Dep. Física de Particulas, E-15706 Santiago de Compostela, Spain

[c] *Permanent address:* Univ-GH-Siegen, Phys. Dept., D-57068 Siegen, Germany

[d] Laboratoire associé au Centre National de la Recherche Scientifique - URA D0063

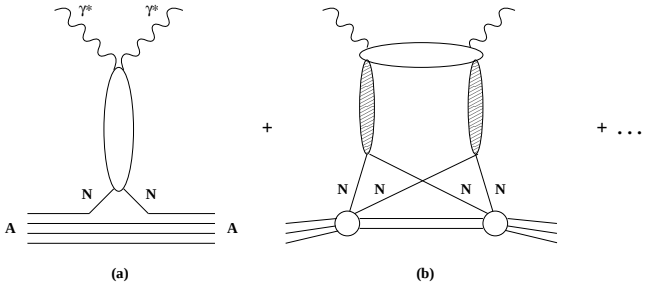

Fig. 2. The first two terms (single and double scattering) of the multiple scattering series for the total $\gamma^* N$ cross-section in the Gribov-Glauber approach

[10], the contribution of the diagram of Fig. 2b to the total $\gamma^* A$ cross-section is related to the diffractive production of hadrons by a virtual photon as follows:

$$\sigma_A^{(2)} = -4\pi\ A(A-1) \int d^2b\ T_A^2(b) \times \int_{M^2_{min}}^{M^2_{max}} dM^2\ \frac{d\sigma^{\mathcal{D}}_{\gamma^* p}}{dM^2 dt}\bigg|_{t=0} F_A^2(t_{min})\ , \quad (1)$$

where $T_A(b)$ is the nuclear profile function, ρ_A is the nuclear density ($T_A(b) = \int_{-\infty}^{+\infty} dZ \rho_A(b,Z)$, $\int d^2b\ T_A(b) = 1$) and

$$F_A(t_{min}) = \int d^2b J_0(\sqrt{-t_{min}}b) T_A(b)\ ,$$

$$t_{min} = -m_N^2\ x^2 \left(\frac{Q^2}{M^2+Q^2}\right)^{-2}\ .$$

Note that $F_A(t_{min})$ is equal to unity as $x \to 0$ and decreases fast as x increases to $x_{cr} \sim \frac{1}{m_N R_A}$, due to a lack of coherence for $x > x_{cr}$.

Equation (1) is written in the approximation $R_A^2 \gg R_N^2$, where R_N is the radius of the $\gamma^* p$ interaction. It will be used in this form only for $A > 20$ (see below). We have also neglected the real part of the Pomeron amplitude which is small for our value of the Pomeron intercept (see (5)). However, for higher values of this intercept the contribution of the real part can be substantial [11].

For a deuteron, the double rescattering contribution has the following form

$$\sigma_D^{(2)} = -2 \int_{-\infty}^{t_{min}} dt \int_{M^2_{min}}^{M^2_{max}} dM^2 \frac{d\sigma^{\mathcal{D}}_{\gamma^* N}}{dM^2 dt} F_D(t) \quad (2)$$

where $F_D(t) = \exp(at)$, with $a = 40$ GeV^{-2}. M^2_{min} in (1), (2) corresponds to the minimal mass of the diffractively produced hadronic system and M^2_{max} is chosen according to the condition: $x_P = x \cdot \frac{M^2+Q^2}{Q^2} \simeq \frac{M^2+Q^2}{W^2} \leq 0.1$.

Equation (2) has been used to calculate inelastic contributions to Glauber corrections in hadron-deuteron interactions [12, 13] and was generalized to heavier nuclei in the form (1) in [14].

Thus the second order rescattering term can be calculated if the differential cross-section for diffractive production by a virtual photon is known.

Higher order rescatterings are model dependent, but calculation shows that, for the values of A and x ($x \gtrsim 10^{-3}$) where experimental data exist, their contribution is rather small. We use the following unitary expression for the total $\gamma^* A$ cross-section

$$\sigma_{\gamma^* A} = \sigma_{\gamma^* N} \int d^2b \frac{A\ T_A(b)}{1 + (A-1) f(x,Q^2) T_A(b)} \quad (3)$$

where

$$f(x,Q^2) = 4\pi \int dM^2\ \frac{d\sigma^{\mathcal{D}}_{\gamma^* p}}{dM^2 dt}\bigg|_{t=0} F_A^2(t_{min}) / \sigma_{\gamma^* N}\ .$$

This expression is valid in the generalized Schwimmer model [15, 16] and is obtained from a summation of fan diagrams with triple Pomeron interaction. However, its physical basis and applicability is much broader. For example it follows from the rescattering of a $q\bar{q}$ system with transverse sizes distributed according to a gaussian [17]. We have checked that the results obtained from a summation of higher order rescatterings of an eikonal type are very similar to the ones obtained with (3) – the differences being of the order of one percent.

Thus we have for the ratio $R_A = F_{2A}/F_{2N}$ of nucleus and nucleon structure functions, in the region of small x

$$\frac{F_{2A}}{F_{2N}} = \int d^2b \frac{A\ T_A(b)}{1 + (A-1) f(x,Q^2) T_A(b)}\ . \quad (4)$$

The deviation of this ratio from $A^1 = A \int d^2b T_A(b)$ is due to the second term in the denominator of the integrand in (4). Thus, knowing the differential cross-section for diffraction dissociation on a nucleon and the structure function of a nucleon ($\sigma_{\gamma^* N}$), one can predict the A (and x, Q^2) dependence of structure functions of nuclei. Equation (4) can only be used in the region of x substantially smaller than 10^{-1} where the sea quarks component dominates. For x close to 10^{-1} shadowing of valence quarks (which in general is not described by (4)) becomes important [18, 19]. The effects leading to antishadowing (such as real parts in the rescattering diagram due to secondary exchanges) are also important in the region of $x \sim 0.1$.

In [4] we described the diffractive contribution to DIS in terms of Pomeron exchange

$$F_2^{\mathcal{D}}(x,Q^2,x_P,t) = \frac{(g^P_{pp}(t))^2}{16\pi} x_P^{1-2\alpha_P(t)} F_P(\beta,Q^2,t) \quad (5)$$

where $g^P_{pp}(t)$ is the Pomeron-proton coupling ($g^P_{pp}(t) = g^P_{pp}(0)\exp(Ct)$ with $(g^P_{pp}(0))^2 = 23$ mb and $C = 2.2$ GeV^{-2}), $\alpha_P(t) = \alpha_P(0) + \alpha'_P(0)t$ is the Pomeron trajectory ($\alpha_P(0) = 1.13$, $\alpha'_P(0) = 0.25$ GeV^{-2}) and $F_P(\beta,Q^2,t)$ is the Pomeron structure function. The variable $\beta = \frac{Q^2}{M^2+Q^2} = \frac{x}{x_P}$ plays the same role for the Pomeron as the Bjorken variable x for the proton. At large Q^2, F_P can be expressed

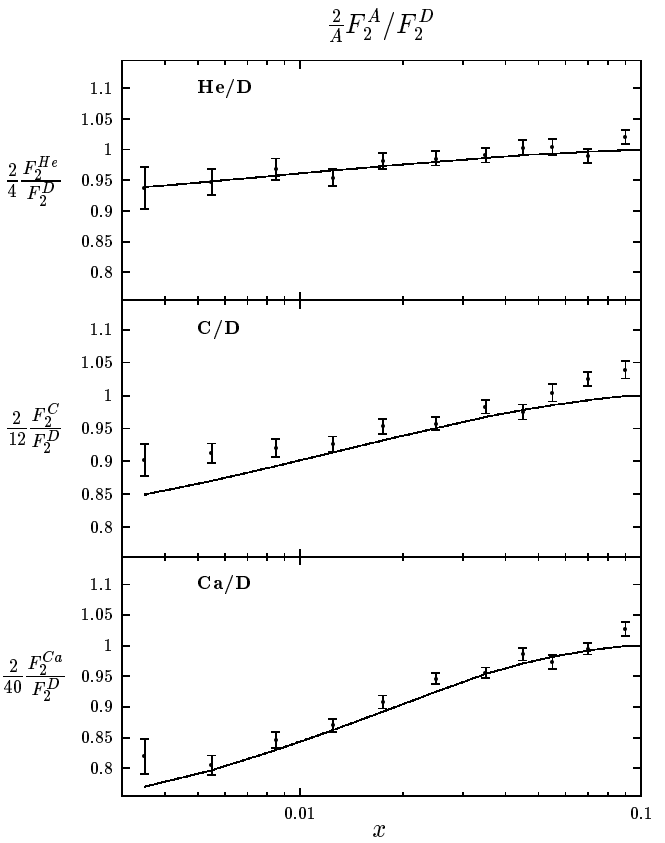

Fig. 3. The ratios $(2/A)F_2^A/F_2^D$ computed from (3) for different values of x. The *experimental points* are from [32]. The values of Q^2 are different for different x-values [32]

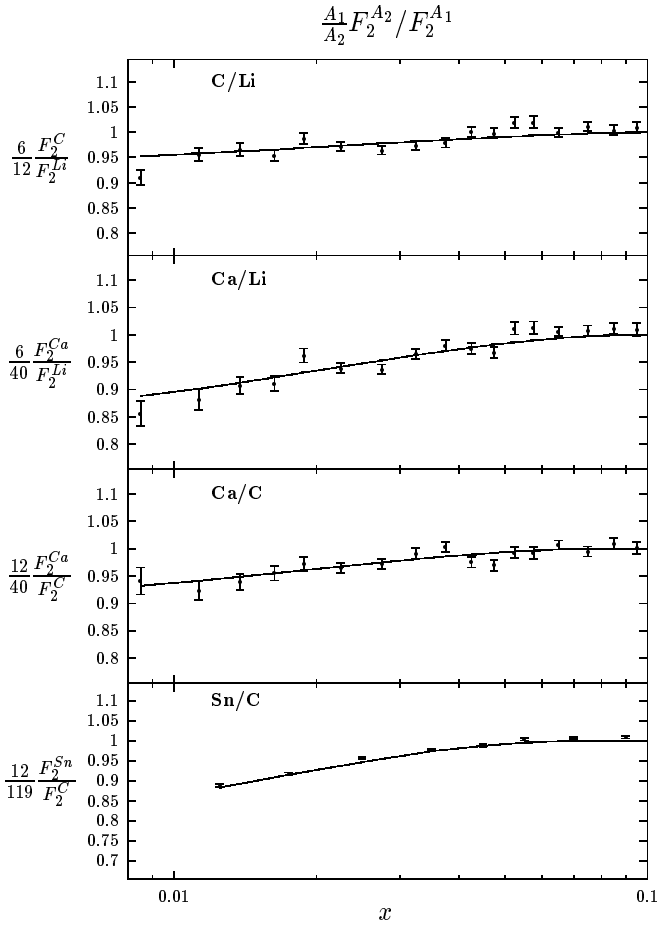

Fig. 4. The ratios $(A_1/A_2)F_2^{A_2}/F_2^{A_1}$ computed from (3) for different values of x. The *experimental points* are from [32] and [33]. The values of Q^2 are different for different x values [32, 33]

in terms of the quark distributions in the Pomeron

$$F_P(\beta,Q^2,t)=\sum_i e_i^2\beta\left[q_i^P(\beta,Q^2,t)+\bar{q}_i^P(\beta,Q^2,t)\right]\ . (6)$$

In [4] we determined $F_P(\beta,Q^2,t)$ using Regge-factorization for small values of β and a plausible assumption on the $\beta\to 1$ behavior. This function was then used as an initial condition for QCD evolution of partons in the Pomeron. The results of the QCD-evolution crucially depend on the form of the gluon distribution in the Pomeron. Experimental results for $F_2^{\mathcal{D}}$ can be understood only if the distribution of gluons in the Pomeron is rather hard and the gluons carry the main part of the Pomeron momentum [4, 20–22]. The explicit forms of all these functions are given in Appendix 1.

The validity of Pomeron factorization (5) for $F_2^{\mathcal{D}}$ as well as that of the QCD evolution for partons in the Pomeron has been questioned in recent papers. These papers deal with diffractive charm production [23, 24] and with the contribution of longitudinal photons to diffractive production [25, 26]. However, in all these papers high-twist effects (in Q^2 or M_Q^2, where M_Q is the mass of the heavy quark), which give small contributions to diffractive cross-sections, were considered. Arguments in favour of usual QCD evolution for the main twist contribution to $F_2^{\mathcal{D}}$ have been given in [27]. In any case the CKMT model [4] gives a reasonable description of diffractive production in DIS. Thus it effectively includes high twist effects and can be used to compute the function $f(x,Q^2)$, which determines the shadowing of nuclear structure function via (4). This function can be written in terms of the ratio F_P/F_{2N}:

$$f(x,Q^2)=\int\frac{d\beta}{4\beta}\left(g_{pp}^P(0)\right)^2\left(\frac{1}{x_P}\right)^{2\Delta}\times\frac{F_P(\beta,Q^2)}{F_{2N}(x,Q^2)}F_A^2(t_{min}) \quad (7)$$

where the integration limits are x/x_{0P} with $x_{0P}=0.1$ and $Q^2/(M_{min}^2+Q^2)$. In the following we take $M_{min}^2=0.4$ GeV^2, in order to include the ρ-meson peak in the integration region.

The parametrization of the Pomeron [4] and nucleon [28] structure functions are given in Appendix 1. Note that the Q^2-dependence of nuclear shadowing is obtained by evolving separately the nucleon and Pomeron structure functions and taking their ratio in (7). Actually, one should compute first F_{2A} at $Q^2=Q_0^2$ and evolve it using

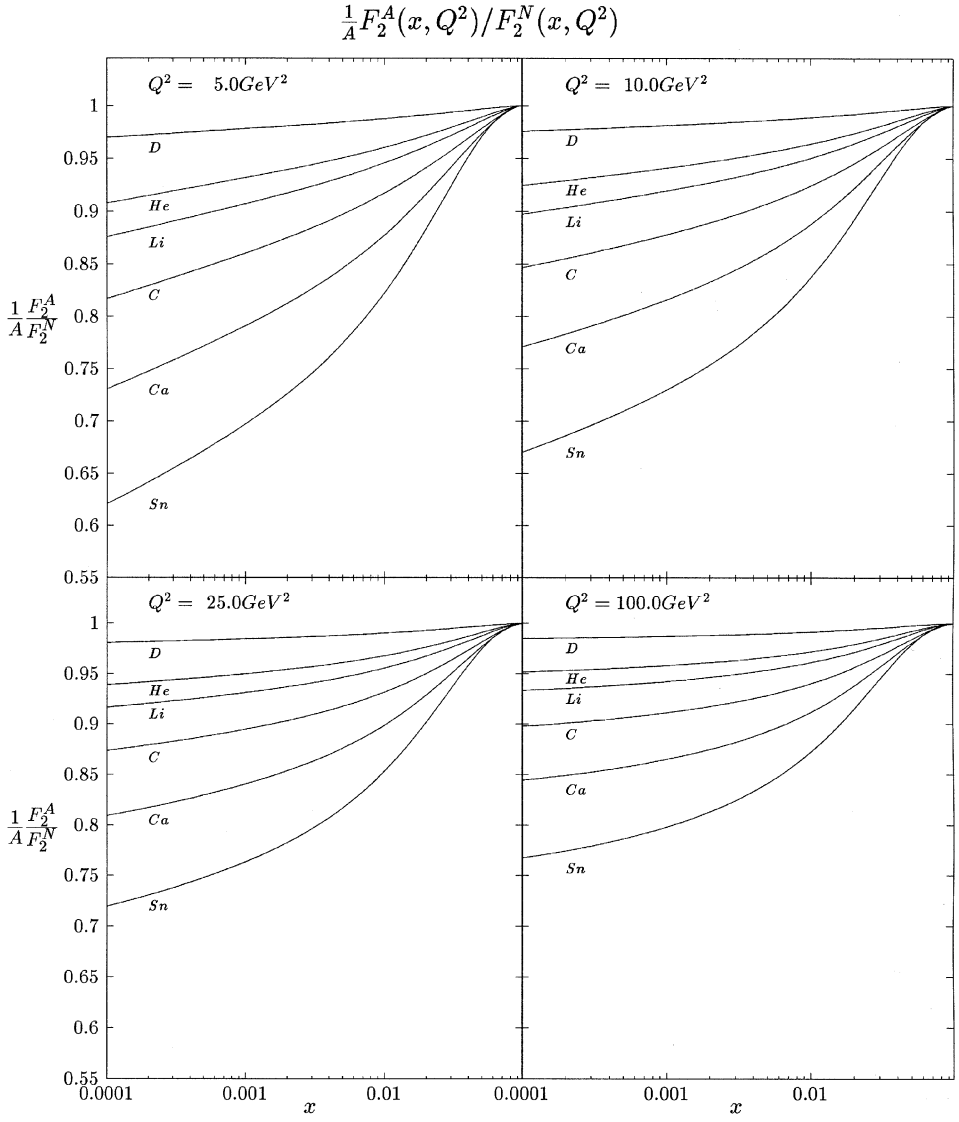

Fig. 5. The ratios $(1/A)F_2^A/F_2^N$ computed from (3) for different values of x in the small x region, at fixed values of Q^2

the nuclear partonic distributions. However, this would require the knowledge of these distributions for all values of x. At small x, where sea quarks are dominant, these two procedures are equivalent for the Born term and the first rescattering correction in (4). As discussed above, higher rescattering corrections are small.

In the numerical calculations we use a standard Woods-Saxon profile $T_A(b)$ for $A > 20$. For light nuclei ($A < 20$) we use a gaussian profile

$$T_A(b) = \frac{3}{2\pi R_A^2} \exp(-3b^2/2R_A^2) \tag{8}$$

with an r.m.s. radius parametrized as [29]

$$R_A = 0.82\ A^{1/3} + 0.58 \text{ fm} \quad . \tag{9}$$

For deuteron (9) is not valid. In this case we use (2). The simple exponential form of $F_D(t)$ gives results which differ by less than 20% from the more sophisticated parametrization used in [6, 30].

In (1) we have neglected the t-dependence of the $\gamma^* p$ diffractive cross-section. As explained above, this approximation is only used for large nuclei where nucleon sizes can be neglected as compared to nuclear ones. For light nuclei ($A < 20$), we take into account this t (or b)-dependence by making the following replacement

$$R_A^2 \Rightarrow R_A^2 + R_N^2 \quad , \qquad R_N = 0.8 \text{ fm} \, . \tag{10}$$

This nucleon radius approximately describes the t-dependence of the $\gamma^* p$ diffractive cross-section in the kinematical region we are interested in.

3 Numerical results

The results of our calculations are shown in Figs. 3–7. Theoretical predictions for the deuteron structure function $F_2^D/2F_2^N$ are shown in Fig. 5. Our results are close to those of [30, 31] but smaller by a factor of about 3 from the results of [6]. Comparison of our predictions for the ratio

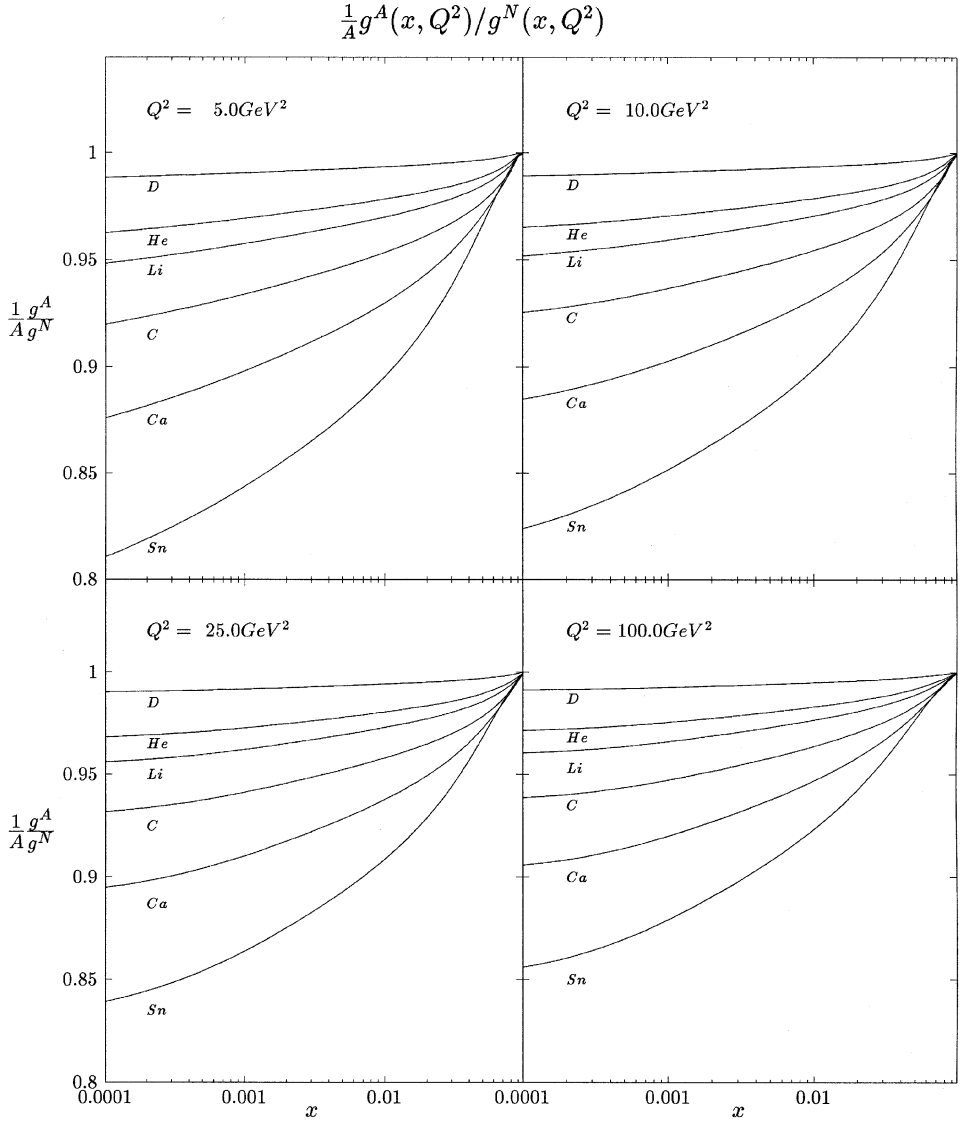

Fig. 6. The ratios $(1/A)g^A/g^N$ of gluon distribution functions computed for different values of x in the low x region, at fixed values of Q^2

$\frac{2}{A}F_2^A/F_2^D$ with experimental data of NMC [32] is shown in Fig. 3 and for ratios of different nuclei in Fig. 4. New data for the ratio F_2^{Sn}/F_2^C [33] are also shown in Fig. 4. It is important to note that experimental points in Figs. 3, 4 for different x correspond to different values of $< Q^2 >$ [32] [33]. This correlation has been taken into account in our calculations. The agreement between theoretical predictions and experimental data is good. Note that there are no free parameters in our calculations.

Our predictions for the ratio $\frac{1}{A}\frac{F_{2A}}{F_{2N}}$ in the region of very small x are shown in Figs. 5 for fixed values of Q^2. They could be confronted to experiment if nuclei at HERA would be available. Note that our results are more reliable for small values of x ($x < 10^{-2}$) where the effects of both valence quark shadowing and antishadowing are negligeable. The curves for shadowing effects in the gluon distribution of nuclei $\frac{1}{A}\frac{g^A(x,Q^2)}{g^N(x,Q^2)}$ are shown in Figs. 6. They look similar to the shadowing for the quark case. However the absolute magnitude of the shadowing is smaller in the gluon case contrary to expectations of some theoretical models [1] but in agreement with [34]. (Note that these results are sensitive to the gluonic distribution in the Pomeron, which is poorly known at present). These predictions can be tested in experimental studies of J/ψ and Υ-production on nuclear targets at RHIC and LHC.

Finally we want to discuss in more detail the Q^2-dependence of the shadowing. Recent NMC data [33] for the ratio of F_2^{Sn}/F_2^C are shown in Fig. 7 as functions of Q^2 for fixed values of x in the small x region. The theoretical curves have a weak dependence on Q^2 and are in reasonable agreement with experiment, although the Q^2 dependence seems stronger in the data especially in the region of small Q^2. At larger values of x the data are practically Q^2-independent. These properties should be checked in future experiments.

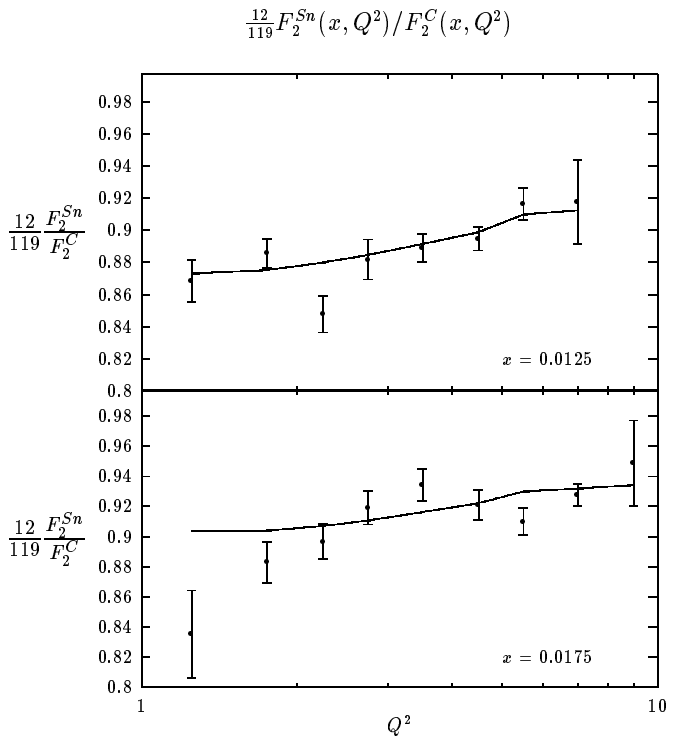

Fig. 7. The ratio $(12/119)F_2^{S_n}/F_2^C$ computed from (3) for different values of Q^2, at two fixed values of x. The *data points* are from [33]

4 Conclusions

In conclusion, a model based on the Gribov-Glauber theory of nuclear shadowing and the properties of diffraction in DIS observed at HERA, leads to a fair description of experimental data on structure functions of nuclei in the small x region. Predictions of shadowing effects for quark and gluon distributions are given. They can be tested in future experiments at HERA and in hadronic colliders.

Acknowledgements. One of us (A.C.) would like to thank G. Do Dang for discussions. A.K. and D.P. wish to thank the LPTHE for hospitality during a period when this work was initiated. This work has been partially supported by grant 93-0079 of INTAS. A.K. also acknowledges support from the grant N° 96-02-19184 of RFFI.

Appendix 1

For the Pomeron and nucleon structure functions we use the parametrization of the CKMT model [4, 28]

$$F_{2N}(x,Q^2) = A(Q^2)x^{-\Delta(Q^2)}(1-x)^{n(Q^2)+4} + B(x,Q^2)x^{1-\alpha_R(0)}(1-x)^{n(Q^2)} \ , \quad \text{(A.1)}$$

$$F_P(\beta,Q^2) = F_{2N}(\beta,Q^2; A \to eA, B(x) \to fB', n \to n-2) \quad \text{(A.2)}$$

where

$$A(Q^2) = A\left(\frac{Q^2}{Q^2+a}\right)^{1+\Delta(Q^2)} \ ,$$

$$B(x,Q^2) = B(x)\left(\frac{Q^2}{Q^2+b}\right)^{\alpha_R}$$

$$\Delta(Q^2) = \Delta_0\left(1+\frac{2Q^2}{Q^2+d}\right) \ ,$$

$$n(Q^2) = \frac{3}{2}\left(1+\frac{Q^2}{Q^2+c}\right)$$

with (all dimensional quantities are in Gev^2)

$$A = 0.1502 \ , \quad B' = 1.2035 \ , \quad \alpha_R = 0.4150 \ ,$$
$$\Delta_0 = 0.07684 \ , \quad a = 0.2631 \ ,$$
$$b = 0.6452 \quad c = 3.5489 \ ,$$
$$d = 1.1170 \ , \quad e = f = 0.07 \ .$$

Finally, we have [28]

$$B(x) = 0.754 + 0.4495(1-x) \quad . \quad \text{(A.3)}$$

The two terms in (A.3) appear because we have used for the valence quark distributions in the proton $d(x) = u(x)(1-x)$. Such a difference between u and d quark distributions is not present in the Pomeron case, and we have dropped the $1-x$ factor in (A.3). In the CKMT model the Pomeron structure function is determined from the nucleon one using triple Regge couplings determined from soft diffraction data and Regge factorization.

Comparison of (A.2) and (6) allows to determine the valence and sea quark distributions in the Pomeron. Likewise one can determine the corresponding ones in the nucleon. These distributions are used as initial conditions at $Q^2 = Q_0^2$ in the DGLAP evolution equation, as described in [28]. The gluon distributions for $Q^2 \le Q_0^2$ in the nucleon and the Pomeron are [4, 28]

$$g^N(x,Q^2) = A_g(Q^2)\ x^{-\Delta(Q^2)}(1-x)^{n(Q^2)+2} \quad \text{(A.4)}$$

$$g_{_P}(x,Q^2) = e\ A_g(Q^2)\ x^{-\Delta(Q^2)}(1-x)^{-0.5} \quad \text{(A.5)}$$

where $A_g(Q^2)$ has the same form as $A(Q^2)$ in (A.1) and (A.2):

$$A_g(Q^2) = A_g\left(\frac{Q^2}{Q^2+a}\right)^{1+\Delta(Q^2)} \quad .$$

The normalization of g^N is obtained from the energy-momentum sum-rule. For the Pomeron this sum-rule is not valid and the normalization of g_P is obtained from that of g^N using Regge factorization. The constant $e = 0.07$ is the same as in (A.2). Actually there is a large ambiguity in the shape of g_P. We have only determined the x-behaviour at small x as well as the absolute normalization. The form (A.5) is just a simple extrapolation to the region of $x \to 1$.

Using the gluon distributions in (4) and (7) one can obtain the corresponding distributions in nuclei.

In order to have exactly the diffractive cross-section computed in [4] as well as the same F_{2N} of [28] we use the values of Q_0^2 in those references. These are $Q_0^2 = 5$ GeV^2 for the Pomeron and $Q_0^2 = 2$ GeV^2 for the nucleon. The corresponding gluon normalizations obtained from the energy-momentum sum rule are $A_g = 1.84$ at $Q_0^2 = 2$ GeV^2 and $A_g = 1.71$ at $Q_0^2 = 5$ GeV^2.

References

1. M. Arneodo, Phys. Reports **240** (1994) 301 (and references therein)
2. V.N. Gribov, ZhETF **56** (1969) 892, ibid **57** (1969) 1306 [Sov. Phys. JETP **29** (1969) 483, **30** (1970) 709]
3. T. Ahmed et al (H1 collaboration), Phys. Lett. **B348** (1995) 681; M. Derrick et al (Zeus collaboration), Z. Phys. **C68** (1995) 569; Z. Phys. **C70** (1996) 391
4. A. Capella, A. Kaidalov, C. Merino, J. Tran Thanh Van, Phys. Lett. **B343** (1995) 403; A. Capella, A. Kaidalov, C. Merino, D. Pertermann, J. Tran Thanh Van, Phys. Rev. **D53** (1996) 2309
5. K. Boreskov, A. Capella, A. Kaidalov, J. Tran Thanh Van, Phys. Rev. **D47** (1993) 219
6. V. Barone et al, Z. Phys. **C58** (1993) 541
7. W. Melnitchouk, A.W. Thomas, Phys. lett. **B317** (1993) 437; Phys. Rev. **C52** (1995) 3373
8. G. Piller, W. Ratzka, W. Weise, Z. Phys. **A352** (1995) 427
9. V.N. Gribov, ZhETF **57** (1967) 654 [Sov. Phys. JETP **26** (1968) 14]
10. V.A. Abramovsky, V.N. Gribov, O.V. Kancheli, Yad. Fiz. **18** (1973) 595 [Sov. J. Nucl. Phys. **18** (1974) 308]
11. A. Bialas, W. Czyz, W. Florkowski, Phys. Rev. **D55** (1997) 6830 and references therein
12. A.B. Kaidalov, L.A. Kondratyuk, JETP Letters **15** (1972) 170; Nucl. Phys. **B56** (1973) 90
13. V.V. Anisovich, L.G. Dakhno, P.E. Volkovitsky, Yad. Fiz. **15** (1972) 168 [Sov. J. Nucl. Phys. **15** (1972) 97]
14. V.A. Karmanov, L.A. Kondratyuk, JETP Letters **18** (1973) 266
15. A. Schwimmer, Nucl. Phys. **B94** (1975) 445
16. K.G. Boreskov et al., Yad. Fiz. **53** (1991) 569 [Sov. J. Nucl. Phys. **53** (1991) 356]
17. B. Kopeliovich et al., JINR E2-86-125
18. L.L. Frankfurt, M.I. Strikman, S. Liuti, Phys. Rev. Lett. **65** (1990) 1725
19. A.B. Kaidalov, C. Rasinariu, U. Sukhatme, UICHEP-TH/96-9
20. T. Gehrmann, W.J. Stirling, Z. Phys. **C70** (1996) 89
21. K. Golec-Biernat, J. Kwiecinski, Phys. Lett. **B353** (1995) 329
22. J. Dainton (H1 collaboration), *Proceedings Workshop on Deep Inelastic Scattering and QCD*, Paris, France, 24-28 April 1995 (ed. J.P. Laporte, Y Sirois)
23. M. Genovese, N.N. Nikolaev, B.G. Zakharov, Phys. Lett. **B378** (1996) 347
24. E.M. Levin, A.D. Martin, M.G. Ryskin, T. Teubner, Z. Phys. **C74** (1997) 671
25. J. Bartels, H. Lotter, M. Wusthoff, Phys. Lett. **B379** (1996) 248; J. Bartels, C. Ewerz, H. Lotter, M. Wusthoff, Phys. Lett. **B386** (1996) 389
26. M. Genovese, N.N. Nikolaev, B.G. Zakharov, Phys. Lett. **B380** (1996) 213
27. A. Berera, D.E. Soper, Phys. Rev. **D53** (1996) 6162
28. A. Capella, A. Kaidalov, C. Merino, J. Tran Thanh Van, Phys. Lett **B337** (1994) 358
29. M.A. Preston, R.K. Bhoduri, *Structure of the Nucleus*, Addison-Wesley, New York 1975
30. W. Melnitchouk, A.W. Thomas, Phys. Rev. **D47** (1993) 3783
31. B. Badelek, J. Kwiecinski, Phys. Rev. **D50** (1994) 4
32. P. Amandruz et al (NMC collaboration), Nucl. Phys. **B441** (1995) 3
33. N. Arneodo et al (NMC collaboration), Nucl. Phys. **B481** (1996) 23
34. K.J. Eskola, Nucl. Phys. **B400** (1994) 240